*Journal of Contemporary Technology and Applied Engineering (JCTAE), **1**(1), 2022, 82-88*

DOI: 10.21608/JCTAE.2022.160264.1010 Published by: *Faculty of Engineering, Kafrelsheikh University*

THE INFRARED SUPPRESSION AND COOLING BY UTILIZING EJECTORS

Received: 02-09-2022
Accepted: 05-09-2022

A.E. Kabeel[a], A.M. El-Zahaby[a], E.A. El-Shenawy[a], A.I. Bakry[a], Z.M. Omara[b]

[a] *Mechanical Power Engineering Department, Faculty of Engineering, Tanta University, Tanta 31734, Egypt.*

[b] *Mechanical Engineering Department, Faculty of Engineering, Kafrelsheikh University, Kafrelsheikh 33516, Egypt.*

[*] corresponding author: Z. M. Omara (zm_omara@eng.kfs.edu.eg)

ABSTRACT. A fluid dynamic pump without moving elements is called an ejector. Traditional ejector systems move energy from a high velocity primary stream to a lower energy secondary stream via viscous forces. Such ejector systems can cool jet engines' exhaust systems and provide IR (Infrared) suppression. In this paper, experiments are carried out to determine the ideal compressible subsonic air ejector design for use as an IR suppression tool. Using the Particle Image Velocimetry (PIV) technique, the flow field of the problem under consideration is experimentally measured. The obtained results provide the best guidance for exhaust ejector design and aid in understanding the flow behaviors and physical phenomena that occur in the flow through ejectors. In addition, the optimum exhaust mixed air temperature is achieved for an ejector with length-to-diameter ratio of $L_E/D_E = 7$, mixing suction to nozzle exit area ratio $AR_E = 36$, and the axial position of primary nozzle relative to the ejector inlet $L_S = - 0.5\ D_E$. Under these conditions the exhaust mixed air temperature reduces by 40% about no ejector case. At this optimum exhaust mixed air temperature; the emissive power is suppressed to 330 %.

KEYWORDS: Infrared suppression, thrust augmenting, two-dimension flow, ejectors of jet engines.

1. INTRODUCTION

A fluid dynamic pump without moving elements is called an ejector. An ejector is seen schematically in Fig. 1. The primary nozzle, intake section, mixing section, and diffuser are the four key components that make up the configuration of the ejector unit. The primary driving fluid's kinetic energy is utilized in the ejector to produce a low-pressure area that entrains the secondary fluid stream. The mixing of the two fluid streams takes place in the ejector's mixing chamber, and the resulting fluid combination is squeezed and released downstream into the diffuser. Compared to the initial primary flow, the exhaust jet that results have a higher flow rate and a lower velocity. Such ejector systems can increase thrust, reduce jet noise, suppress IR, and cool jet engines' exhaust systems. The advantages of the ejector are in its simplicity, ease of use, sturdy construction, lack of moving parts, low maintenance requirements, and lengthy service life. Military operators are aware of the effectiveness of current exhaust ejectors as IR suppressors. For military objectives, a drop in exhaust temperature lowers the exhaust flow's infrared signature. For some combat aircraft, this is advantageous because the exhaust gases give off a lot of infrared radiation, making the aircraft visible. Infrared radiation is decreased by lowering the temperature of the exhaust gas. Toulnay, F. [1] tested an exhaust ejector twin-engine helicopter and found that the suppressors reduce the IR radiation emitted by the hot parts. Birk and Davis [2] tested an exhaust ejector for naval applications. Also, Power et al. [3] used the ejectors to minimize infrared radiation signals for military aircraft. Additionally, many warships, including frigates, cruisers, and even aircraft carriers, are propelled by gas turbine engines in the navies of more than two dozen different nations. According to Birk and Davis [4], it is crucial to pay close attention to the fighters, tanks, and even commercial ships' low heat (i.e., infrared) signature and quietness.

The scientists and engineers working on this technology have struggled with how to cool the parts that come into contact with the hot exhaust gases from engines without suffering an unbearable

performance loss. The ejectors are also applied in gas turbine engines test cells as efficient cooling devices instead of using forced cooling systems. The cooling of the tail pipe and nozzle of jet engine is enhanced by providing an extension cooling concept that includes variable area and length ejectors. The entrainment air used to cool the surfaces upstream of the ejector (the tail pipe and nozzle) to avoid overtemperature of the components. The air ejector as a simple, light-weight unit for pumping cooling air is promising solution to the high temperature problems. Presz and Michael [5] set several ejector pumps in series. Their results indicate that, the new device generates higher diffusion rates and more efficient wall cooling.

In order to increase pumping performance and augment thrust, ejector nozzles have been developed in conjunction with unique mixer nozzles [6]. The primary nozzle's mixing capacity is investigated using both computational and experimental methods because this is the key to improving the performance of the ejector. Military reconnaissance and target drones like the Airbus Do-DT-25 are the main applications for very small turbojet engines outside of model aircraft propulsion. Future applications will place even higher demands on propulsion systems, such as autonomous area reconnaissance or air cargo delivery [7]. As a result, relatively compact turbojet engines must be upgraded for both aircraft integration and their low overall efficiency (5-10% [8]). In order to increase thermal efficiency, a greater pressure ratio and higher turbine inlet temperature are required.

The mixing of the primary and secondary streams is a problem that makes the ejector idea extremely difficult to operate. Incomplete mixing results in a variety of loss processes. To reduce the size and weight penalty the engine imposes, this mixing must be accomplished in the shortest amount of time.

The previous literatures have not obtained the optimum configurations of exhaust ejectors to give to give minimum exhaust mixed air temperature and or for nozzle and tail pipe based on the effect of the variation of all geometrical and operational parameters. So that, the aim of this paper is to determine the optimum configurations of exhaust ejectors to give minimum exhaust mixed air temperature (IR suppression) without losses of thrust. The design of ejectors is a complex problem; many operational and geometrical parameters can affect performance of ejector. These factors include: ejector length-to-diameter ratio (L_E/D_E), ejector area ratio (AR_E), the axial position of primary nozzle relative to the ejector entry (L_S), total temperature of primary jet (T_P) and nozzle pressure ratio ($p_{op}/p_{atm.}$), as shown in Fig. 1.

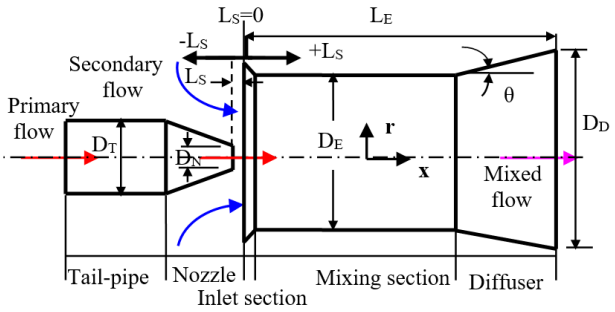

Fig. 1. Definition of ejector geometry with conventional nozzle.

2. THE EXPERIMENTAL SETUP

The experimental investigation was conducted using an open aerodynamic circuit. The experimental test rig is shown schematically in Fig. 2. The experimental facility consists of two reciprocating compressors which compress air to air tank. Each compressor is driven by an electric-motor having an output power of 7.5 kW. Through a compressed air line, air is delivered from the tank to the settling pipe. A valve installed downstream of the tank is used to control the primary air mass flow rate ($\dot{m}_P$), whereas it is measured by orifice meter mounted within the settling pipe. The settling pipe was connected to a settling chamber through a divergent section. The settling chamber supports the heaters and screens. Each heater is a cylindrical shape bar of diameter 6 mm and one-meter length generates a thermal power about 1 kW. A convergent section connects the settling chamber to the tail pipe. A tail pipe carries the air from the settling chamber to the convergent nozzle. The K-type thermocouple is supported in the first of tail pipe wall to measure the total temperature of the primary air. The air flowing through the nozzle is exhausted to ejector and finally into the atmosphere. The K-type thermocouples are supported a long tail pipe and nozzle walls to measure the temperatures of the primary air, tail pipe wall and nozzle wall. The air exiting the nozzle was exhausted through the ejector before being released into the atmosphere and the temperature of exhaust air are measured using four thermocouples.

Two Pitot-static tube are used whereas the first mounted upstream of nozzle (mid of the tail pipe) to measure the total pressure. The second Pitot-static tube is located at the centerline of the exit nozzle, to measure the velocity and static pressure of primary air. The used Pitot-static tubes are calibrated with standard Pitot-static tube. The primary jet of air entrains additional air from the surroundings and discharges the mixture of primary jet and entrained air (secondary air) through the ejector to the atmosphere. For determination of the secondary air mass flow rate, the tail pipe, nozzle and entrance part of ejector are mounted inside entry chamber, which is

a box made of Perspex. The secondary air is drawn from four holes in upstream side of entry chamber. These holes are symmetrical with respect to the tail pipe and connected to a secondary flow pipe via four tubes. The mass flow rate of the secondary flow ($\dot{m}_S$) is measured by orifice meter mounted within secondary flow pipe. The air flow field through the ejector is measured in meridional plane using Particle Image Velocimetry (PIV).

An experimental investigation of the effect of geometrical and operational parameters variations on the exhaust mixed air temperature for nozzle and tail pipe of ejector with and without diffuser is presented. The ejectors are made of transparent Perspex in order to measure the air flow field from outside surface of the ejectors using PIV. Ejectors have cylindrical mixing sections of length-to-diameter ratios (L_E/D_E) varied from 2 to 13 and ejector area ratio (AR_E) from 11 to 75. Convergent nozzle with 50 mm length and has area ratio 11.1 is used. The series of computations and experiments are repeated for nozzle pressure ratio ($p_{op}/p_{atm.}$) varying from 1.1 to 1.8. The axial position of primary nozzle relative to the ejector inlet (L_S) varied from - 2 D_E (the nozzle outside the ejector) to 2 D_E (the nozzle inside the ejector) and total temperature of primary jet (T_P) varying from 300 to 600 K.

The Spectral emissive power (E_λ) can be calculated from Plank's formula:

$$E_\lambda = \frac{C_1 \lambda^{-5}}{\left(e^{C_2/\lambda T} - 1\right)} \quad W/m^2.\mu m$$

Where,

$C1 = 3.742 \times 108$, W. $\mu m^4 / m^2$

$C2 = 1.4387 \times 104$, $\mu m . K$

λ = Wave length, μm

T = Average temperature of air, K

The following parameters are used: -

a- Exhaust temperature ratio defined as (T_{Ee}/T_{Ne}) as a measure of IR signature suppression.

Where,

T_{Ee}= Average exhaust mixed air temperature at ejector exit, (K)

T_{Ne}= Average primary air temperature at nozzle exit without ejector, (K)

b- Nozzle wall temperature ratio defined as (T_{Nw}/T_{Nwl}) and Tail-pipe wall temperature ratio defined as (T_{Tw}/T_{Twl}) as a measure of exhaust system cooling.

Where,

T_{Nw}= Average nozzle wall temperature with ejector, (K)

T_{Nwl} = Average nozzle wall temperature without ejector, (K)

T_{Tw}=Average tail pipe wall temperature, with ejector (K)

T_{Twl} = Average tail pipe wall temperature without ejector, (K)

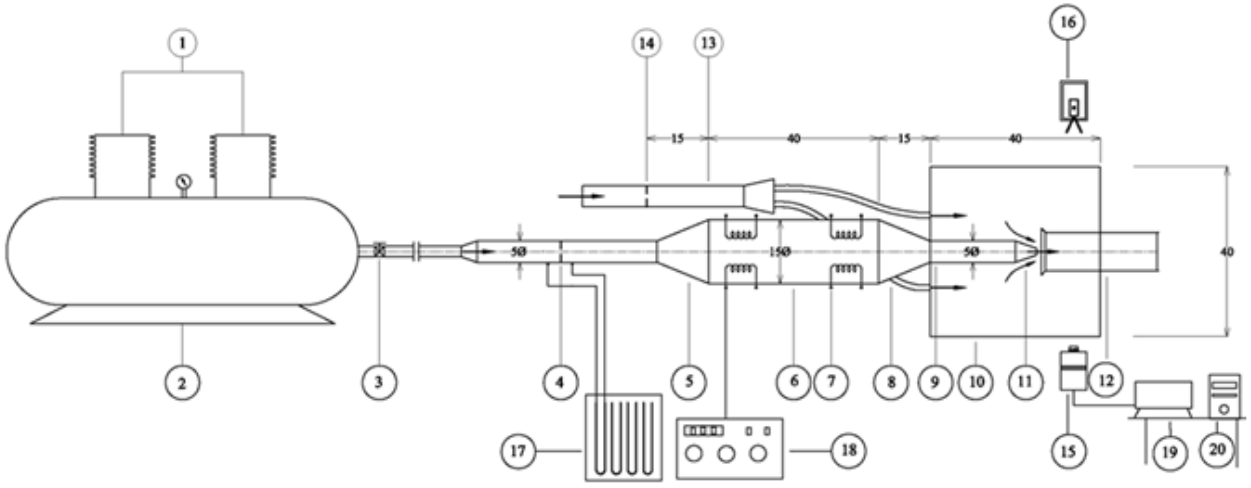

1-Reciprocating compressors	5- Divergent section	9 - Tail pipe	13- Secondary flow pipe	17- Manometers
2- Air pressure tank	6- Settling chamber	10- Entry chamber	14- Secondary orifice	18-Control panel
3- Control valve	7- Heaters	11- Nozzle	15- CCD Camera	19-Monitor
4- Primary orifice	8- Convergent section	12- Ejector	16-Laser power supply	20- CPU

Fig. 2. Experimental test rig

3. RESULTS AND DISCUSSION

In the following section, the results of average exhaust mixed air temperature reduction (IR signature reduction) and reduction of walls temperatures for nozzle and tail pipe at different operating parameters including: nozzle total to static pressure ratio ($p_{op}/p_{atm.}$), total temperature of primary air (T_P), nozzle axial position with respect to ejector entry section (L_S) and mentioned ejector configuration are presented.

3.1. EXHAUST TEMPERATURE RATIO (T_{Ee}/T_{Ne})

The effects of geometrical parameters of the ejector performance are studied at the selected nominal operating parameters. These nominal operating parameters are nozzle pressure ratio $p_{op}/p_{atm.}$=1.5 and nozzle axial position with respect to ejector entry section L_S= 0.

3.1.1. EFFECT OF EJECTOR GEOMETRY ON EXHAUST TEMPERATURE RATIO.

The ejector geometry depends on both ejector length to diameter ratio (L_E/D_E) and area ratio (AR_E). Fig. 3 indicates the variation of average mixed air temperature (T_{Ee}) at ejector exit with ejector length to diameter ratio (L_E/D_E) at different total temperature of primary air (T_P). Fig. 3 shows that, the exhaust temperature (T_{Ee}) decreases continuously as the length of the ejector increases, due to the increased mixing process, where the secondary mass flow rate increases with increasing ejector length to diameter ratio, Fig. 4. The same result was previously obtained by Whitley, N. et. al. [9]. And the exhaust temperature ratio decreases to L_E/D_E=7 after it decreases slowly with increasing ejector length to diameter ratio. Since, the higher length gives higher size and weight of ejector and gives more drag, so that The cylindrical length to diameter ratio corresponding minimum exhaust temperature is L_E/D_E=7 may be considered as an optimum value.

It is appeared also from Fig. 4 that, the mass entrainment ratio ($\dot{m}_S / \dot{m}_P$) increases with increasing length to diameter ratio approximately up to L_E/D_E = 9, and then further increasing of length to diameter ratio nearly has no effect on secondary air entrained, where the mass entrainment ratio approximately remains constant from L_E/D_E = 9 to L_E/D_E = 11 and then decreases slowly for further increasing in ejector length. The entrainment ratio increases with increasing length to diameter ratio, since increasing the length of ejector lead to decreases the static pressure at the ejector entrance which in turn increases the acceleration of surrounding fluid, as shown in Fig. 5. In addition, it can be noticed from Fig. 3 that, the rate of decreasing of average exhaust temperature ratio (T_{Ee}/T_{Ne}) increases with primary air temperature. Where, the results indicate that, increasing the primary air temperature causes a significant increase in jet velocity and create more pressure drop at ejector inlet, which increases the entrained mass flow rate.

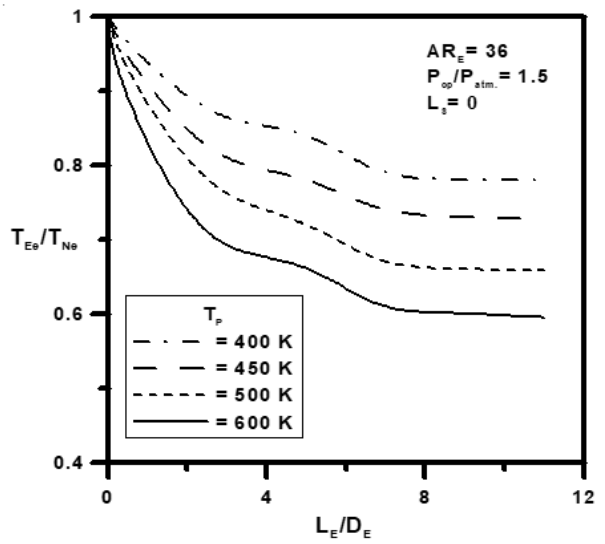

Fig. 3. Effect of L_E/D_E on T_{Ee}/T_{Ne} for AR_E = 36 at different T_P.

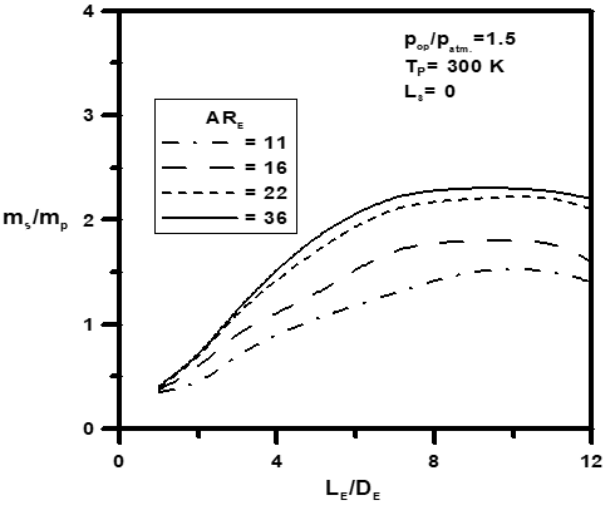

Fig. 4. Effect of L_E/D_E on m_s/m_p at different AR_E.

3.1.2. EFFECT OF EJECTOR AREA RATIO ON EXHAUST TEMPERATURE RATIO.

Fig. 6 indicates the calculated variation of average exhaust temperature with ejector area ratios (AR_E). The results indicate that, the trend of the variation of exhaust temperature with ejector area ratios is opposite to that of the mass entrainment ratio (m_s/m_p), Fig. 4. Where, the mass entrainment ratio increases with increasing area ratio of ejector approximately up to AR_E= 36 and then decreases slowly for further increasing in area ratio of ejector, but the exhaust temperature decreases with increasing area ratio of ejector approximately up to

AR_E = 36 and then increases slowly for further increasing in area ratio of ejector, as shown in Fig. 6. So the ejector area ratio corresponding minimum exhaust temperature AR_E = 36 may be considered as an optimum value. Where, the mass entrainment ratio (m_s/m_p) is maximum value.

Finally, minimum exhaust temperature was obtained when the ejector has area ratio about AR_E = 36 and length to diameter ratio about L_E/D_E= 7, at different primary air temperatures. Under these conditions table 1 shows the values of exhaust temperature ratio (T_{Ee}/T_{Ne}) at different primary air temperatures.

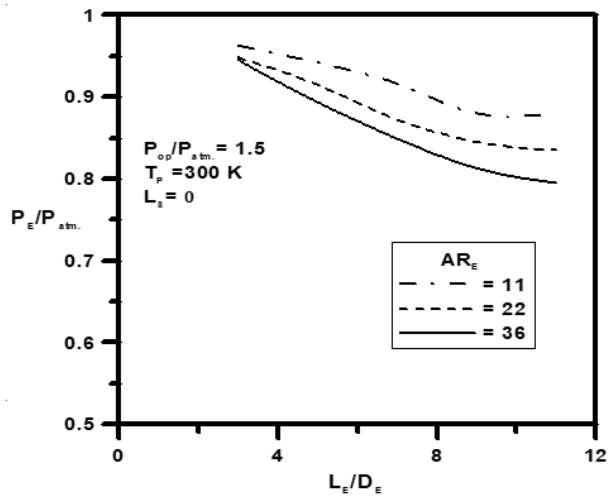

Fig. 5. Effect of L_E/D_E on static pressure at entrance of different ejector.

Table 1 The values of exhaust temperature ratio (T_{Ee}/T_{Ne}) at different primary air temperatures (T_P) for AR_E = 36 and L_E/D_E= 7.

T_P (K)	300	400	450	500	600
T_{Ee}/T_{Ne}	1	0.805	0.730	0.665	0.620

From PIV velocity measurements, Fig. 7 show half section of the velocity vector maps in the entrance of different ejector area ratios at L_E/D_E= 7. It can be indicated from this figure that, the secondary mass flow rate increases with increasing the ejector area ratio.

3.2. EFFECT OF NOZZLE PRESSURE RATIO (POP/PATM.) ON EXHAUST TEMPERATURE RATIO.

Fig. 8 shows how the exhaust temperature ratio (T_{Ee}/T_{Ne}) of the exhaust flow varies with the nozzle pressure ratio (p_{op}/p_{atm}). It can be observed from this figure that, the exhaust temperature ratio increases with nozzle pressure ratio at all temperatures of primary air (T_P). The last observation is due to that the increasing primary mass flow rate is large than the secondary mass flow rate with increasing primary pressure. Also, Fig. 8 shows the increasing exhaust temperature ratio is higher with higher temperatures of primary air (T_P).

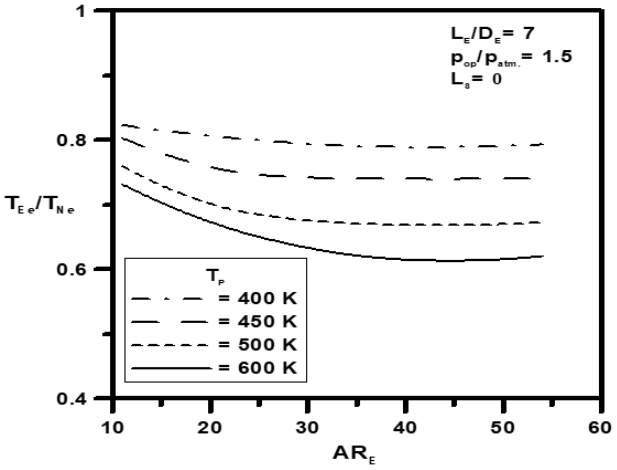

Fig. 6. Effect of AR_E on T_{Ee}/T_{Ne} for L_E/D_E= 7 at different T_P.

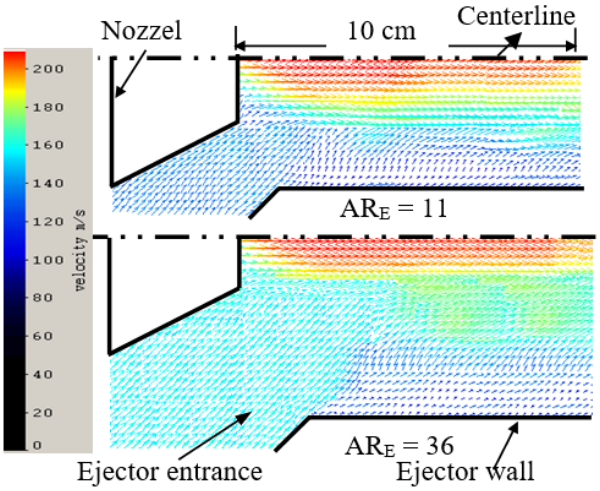

Fig. 7. The half section of the velocity vector maps in the entrance of AR_E = 11 and 36.

3.3. EFFECT OF NOZZLE AXIAL POSITION (L_S) ON EXHAUST TEMPERATURE RATIO.

Fig. 9 shows the effect of varying the axial position of the nozzle relative to the ejector entry with ejector area ratio AR_E= 36 for a fixed nozzle pressure ratio of 1.5, on the exhaust temperature ratio (T_{Ee}/T_{Ne}) of the exhaust flow. The axial distance of the nozzle L_S has negative value when the nozzle is outside the ejector, while L_S is positive as the nozzle becomes inside the ejector. It can be seen that the optimum position occurs when the nozzle is outside the ejector approximately at L_S= -0.5D_E.

The results indicate that, when the position of the nozzle exit is outside the ejector entry by about L_S= -0.5D_E the static pressure at ejector entry has minimum value compared to others position of nozzle. So that the amount of entrainment air is maximum at this

position, Fig. 10, and consequently the exhaust temperature ratio has an optimum value.

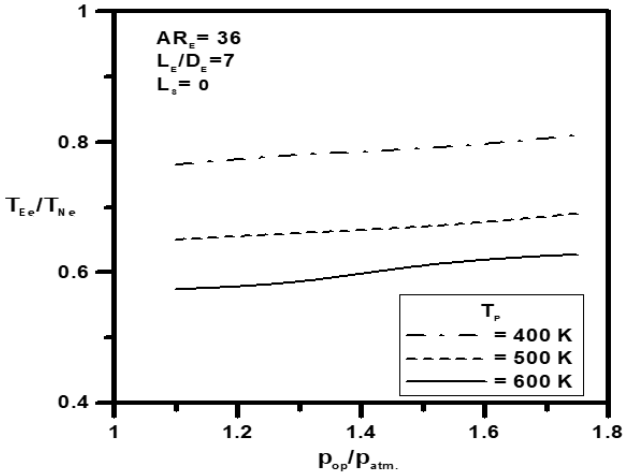

Fig. 8. Effect of p_{op}/p_{atm} on T_{Ee}/T_{Ne} for AR_E =36 L_E/D_E= 7,at different T_P.

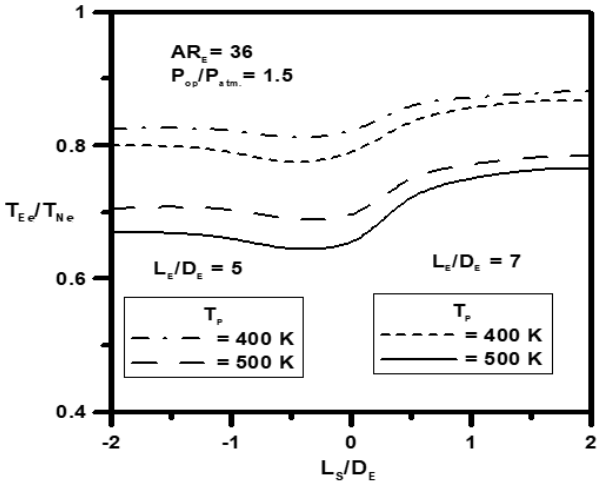

Fig. 9. Effect of L_S/D_E on T_{Ee}/T_{Ne} for AR_E = 36, L_E/D_E= 5 and 7, at different T_P.

3.4. THE SPECTRAL EMISSIVE POWER (E_λ)

A decrease in the exhaust temperature reduces the infrared signature of the exhaust flow. Fig. 11 shows the spectral emissive power (E_λ) with and without ejector, whereas the vertical axis shows the spectral emissive power (E_λ), while the horizontal axis represents the wave length (λ). As shown in Fig. 11, the spectral emissive power decreases in the presence of the ejector, and as the area under curves represent the energy emission then the area between the curves represents the reduction in energy emission.

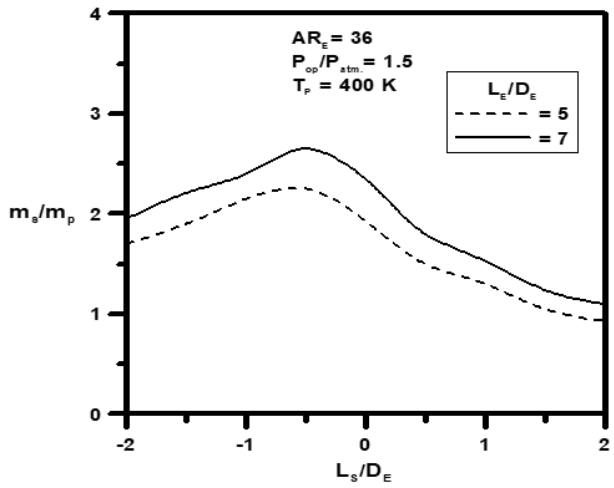

Fig. 10.Effect of L_S/D_E on m_s/m_p for AR_E = 36, L_E/D_E = 5 and 7.

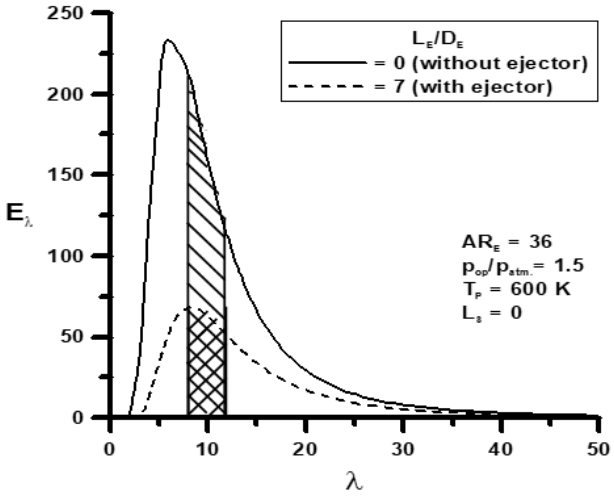

Fig. 11. Infrared emission (E_λ)

4. CONCLUSIONS

To determine the best design for subsonic air ejectors, an experimental investigation is being done to give minimum exhaust mixed air temperature (IR suppression) and minimum wall temperature for nozzle and tail pipe. The following results at total temperature of primary air T_P = 500 K and nozzle pressure ratio $p_{op}/p_{atm.}$=1.5 are obtained:-

1- The optimum exhaust mixed air temperature is reached for an ejector with length-to-diameter ratio L_E/D_E = 7, mixing suction to nozzle exit area ratio AR_E = 36, and the axial position of primary nozzle relative to the ejector inlet L_S = -0.5 D_E. Under these conditions the exhaust mixed air temperature reduces by 40% about no ejector case. At this optimum exhaust mixed air temperature; the emissive power is suppressed to 330 %.

2- The optimum nozzle cooling is achieved at an ejector with length-to-diameter ratio L_E/D_E = 7, mixing suction to nozzle exit area ratio AR_E =

36. Under these conditions the nozzle wall temperature reduces by 23 % about no ejector case,

3- The optimum tail pipe cooling is obtained at an ejector with length-to-diameter ratio $L_E/D_E = 7$, mixing suction to nozzle exit area ratio $AR_E = 36$, Under these conditions the tail pipe wall temperature ratio reduces by 25.6% about no ejector case.

REFERENCES

[1] Toulnay, F. Internal Aerodynamic of InfraRed Suppressors for Helicopter Engines. J. American Helicopter Socity, 33(4), 1-51, 1988.

[2] Birk, A.M., and VanDam, D. InfraRed Signature Suppressing for Marine Gas Turbines: Comparison of Sea Trial and Model Test Results foe the DRES Ball IRSS system. J. Eng. Gas Turbine and Power, . 116, 75-81, 1994

[3] Power, G.D, McClure, M.D. and Vinh, D., "Advanced IR Suppressor Design Using a Combined CFD/Test Approach. AIAA 3215-1994.

[4] Birk, A.M., and Davis, W.R. Suppressing the Infra-Red Signature of Marine Gas Turbines. J. Eng. Gas Turbine and Power, 111, 123-129, 1988.

[5] Presz, Jr., W. and Michael W.T. Multi-Stage Mixer/Ejector Systems. AIAA 2002-4064, 38th AIAA/ASME/SAE/ASEE Joint Propulsion Conference & Exhibit, Indianapolis, Indiana, 7-10 July 2002.

[6] Schmidt R., A Hupfer. Design and numerical simulation of ejector nozzles for very small turbojet engines. CEAS Aeronautical Journal 2021. https://doi.org/10.1007/s13272-021-00537-3.

[7] Nelson, J., Dix, D.: Development of engines for unmanned air vehicles: Some factors to be considered. In: Institute for Defence Analyses, IDA Document D-2788, Alexandria (2003).

[8] A. Hupfer, Hirndorf, D. Investigation of parameters affecting thermodynamic cycle of very small jet engines. In: Proceedings of 15th International Symposium on Transport Phenomena and Dynamics of Rotating Machinery (ISROMAC-15), Honolulu (2014)

[9] Alperin, M. and Wu, J. J. Thrust Augmenting Ejectors, Part I. AIAA Journal, 21, 10, 1428-1436, 1983.

[10] Alperin, M. and Wu, J. J. Thrust Augmenting Ejectors, Part II. AIAA Journal, 21, 12, 1428-1436, 1983.

[11] EL-Banna, R.A.M. New Concepts in Thrust Augmentor Ejectors. SECOND A.S.A.T. Conference 21-23 April 1987, Cairo-Egypt.

[12] Whitley, N., Krothapalli, A. and Van Dommelen, L. A Determinate Model of Thrust-Augmenting Ejectors. Theoretical and Computational Fluid Dynamics, 8:37-55, 1996.

[13] Patankar, S. V. Numerical Heat Transfer and Fluid Flow. Hemisphere Publishing Company, New York, 1980.

[14] Launder, B. E. and Spalding, D. B. The Numerical Computation of Turbulent Flows. Computer Methods in Applied Mechanics and Engineering, 3:269-289, 1974.